

The kinetics of ferrite growth in Fe-C-Mn-Si using controlled decarburization experiments

^aC. Qiu, ^bH. Zurob and ^aC. R. Hutchinson

^a Dept of Materials Engineering, Monash University, Australia

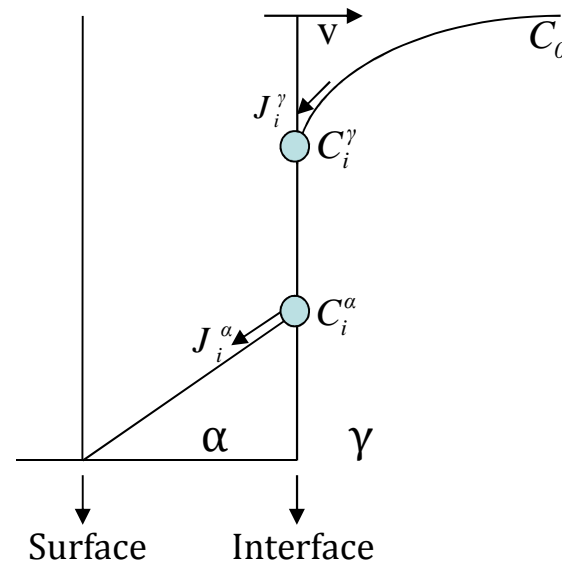
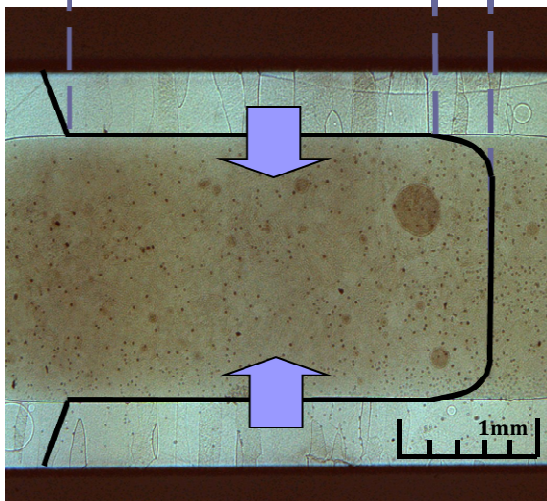
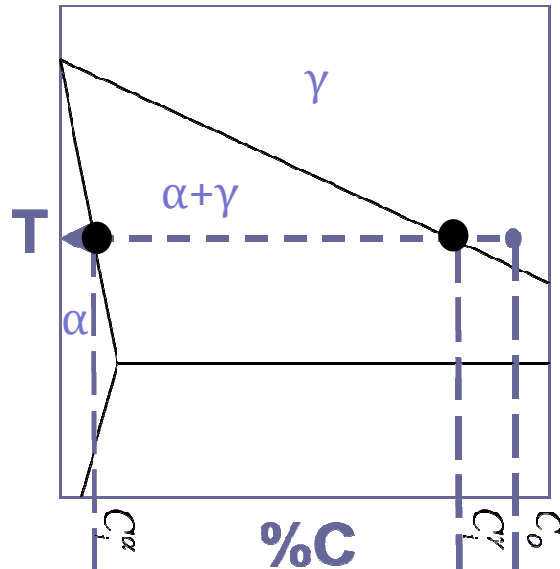
^b Dept of Materials Science & Engineering, McMaster University, Canada

Acknowledgement: International Postgraduate Research Scholarship.
Monash Graduate Scholarship.

Outline

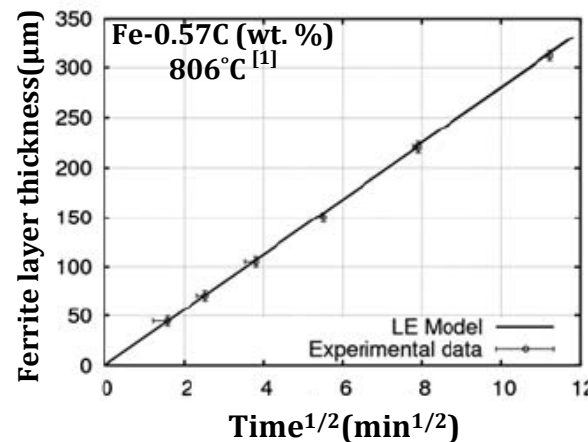
- Advantages and disadvantages of decarb experiments
- Objective – predicting ferrite growth in quaternary and higher order systems
- Alloy systems: Fe-C-Si, Fe-C-Mn & Fe-C-Si-Mn
- Experimental & modelling results
- Summary/Discussion points

Background: Decarburization technique



$$v_t = \frac{J_i^\alpha - J_i^\gamma}{C_i^\gamma - C_i^\alpha}$$

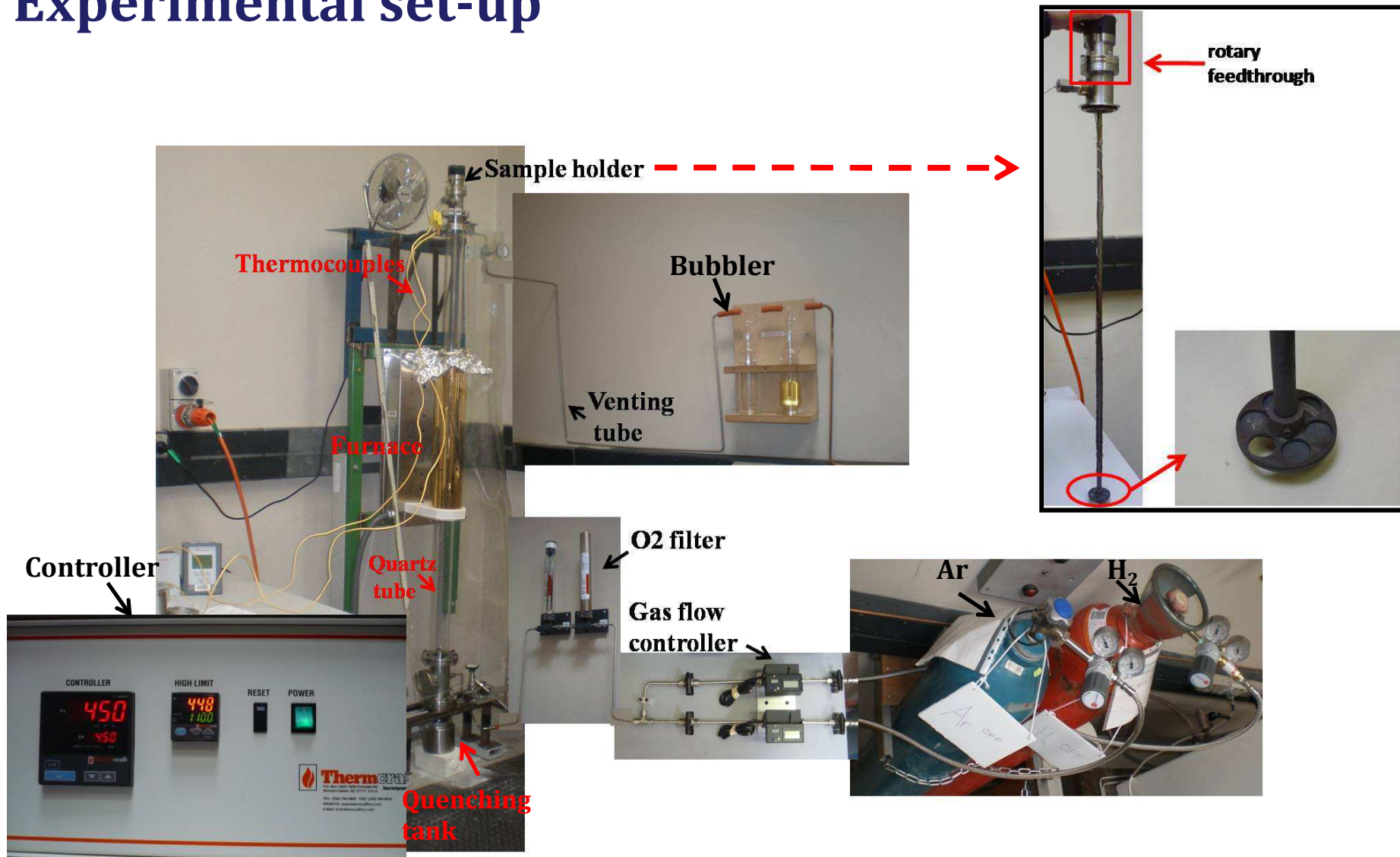
Local equilibrium assumption



- Decarburization generates high quality data for model comparison

- The interface is stabilised to the simple planar geometry

Experimental set-up



Objective of the study

Ferrite growth in Fe-C-X steels is usually used to test models of growth (e.g. those including solute drag).

Solute drag models contain parameters such as the binding energy and the trans-interface diffusivity that are currently difficult to predict. They can be 'tuned' using Fe-C-X kinetic experiments.

The objective of this study is to test how well we can predict the kinetics of growth in higher order systems (Fe-C-X-Y) using parameters tuned from ternary systems

Selected Fe-C-X-Y literature

- Tanaka *et al.* (1995)^[2]: LE and PE phase boundaries for quaternary systems (Mn+(Si,Ni,Co)) calculated using the Central Atoms method.
- Aaronson *et al.* (2004)^[3]: *Coupled Solute Drag Effect* – enhanced accumulation at interfaces due to strong C-X(Y) and/or X-Y interactions leading to enhanced SD effects
- Guo *et al.* (2006, 2007): A C-SDE was used to rationalize the kinetics of ferrite growth, and the transitions to different stages of growth in Fe-C-Mn-Si alloys^[4,5].

[2] Tanaka T, Aaronson HI, Enomoto M, MMTA 1995;26A:561-80

[3] Aaronson HI, Reynolds WT, Purdy GR, MMTA 2004;35A:1187-1210

[4] Guo H, Enomoto M. MMTA 2007;38A:1152-61

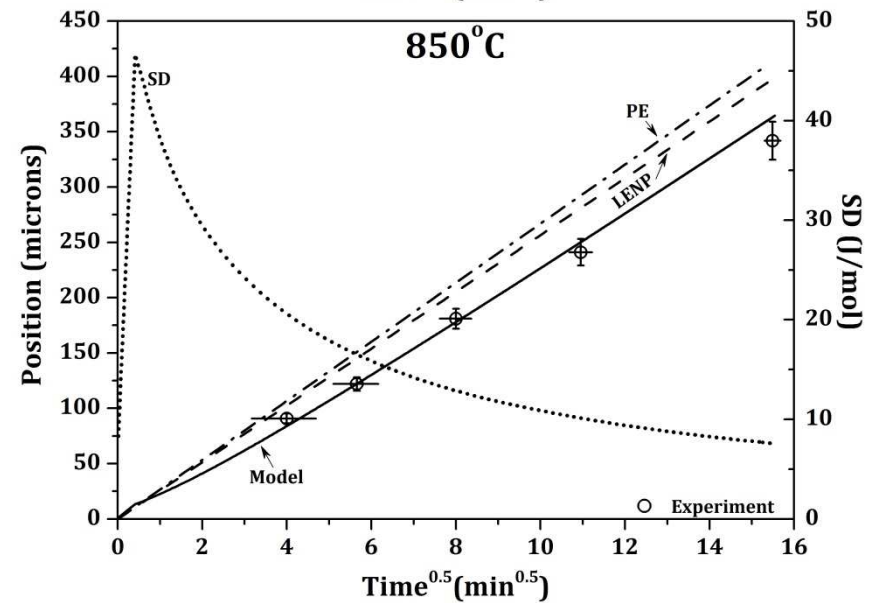
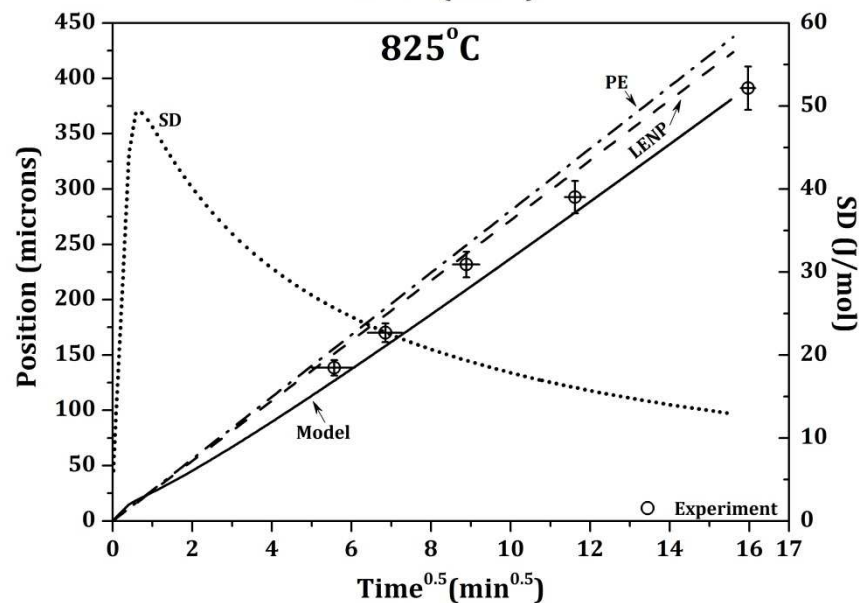
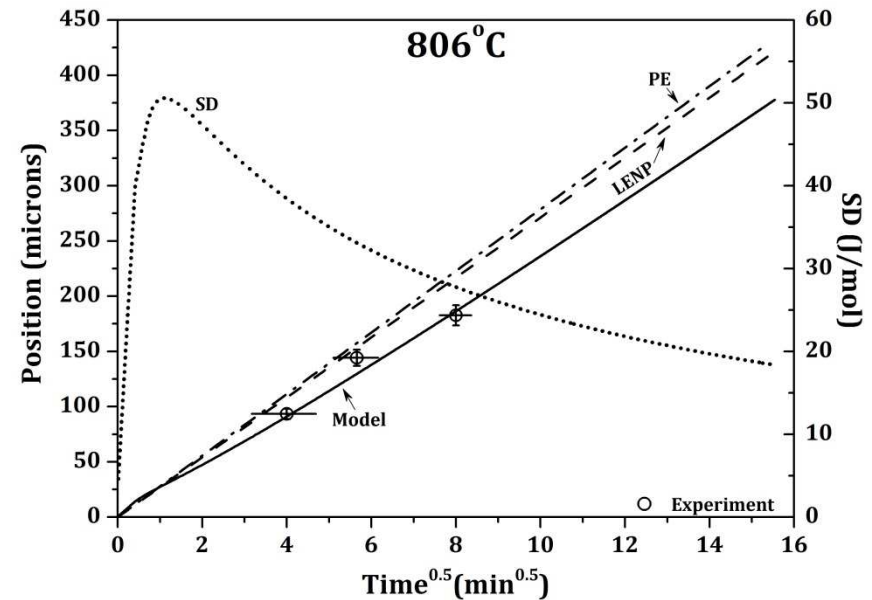
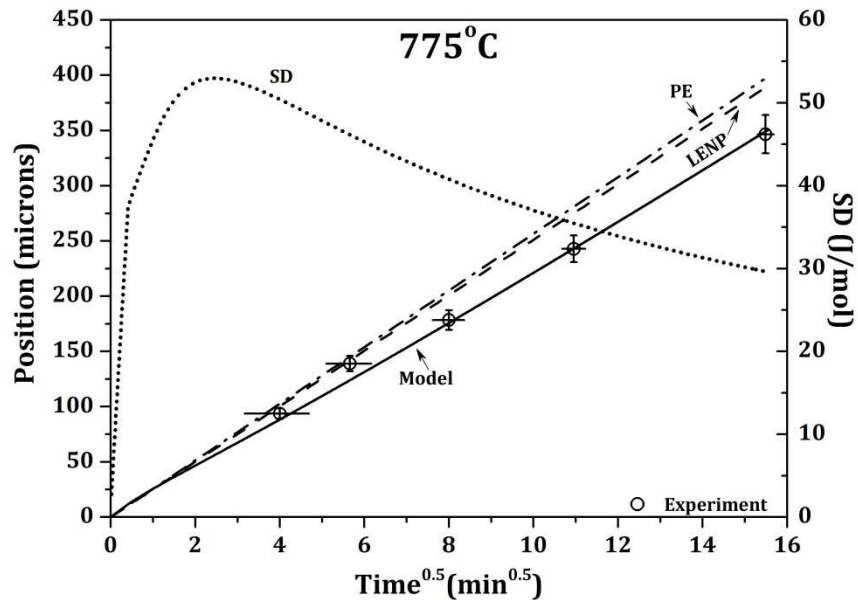
[5] Guo H, Purdy GR, Enomoto M, Aaronson HI, MMTA, 2006;37A:1721-1729

Alloy compositions

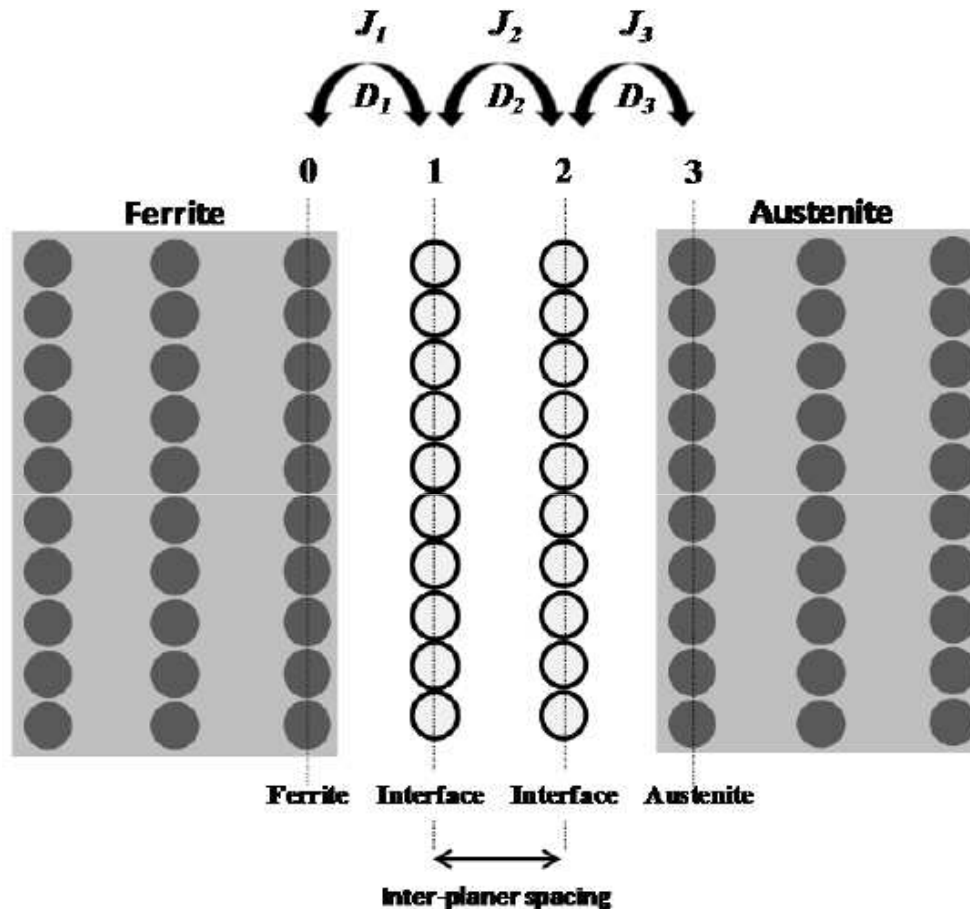
Alloy Composition (wt.%)	Decarburization temperatures (°C)
Fe-0.74C-0.45Si	775, 806, 825, 850
Fe-0.76C-0.84Si	
Fe-0.75C-1.46Si	825, 850
Fe-0.53C-0.47Mn	765
Fe-0.50C-0.53Mn	830
Fe-0.57C-0.94Mn	755, 775, 806, 825
Fe-0.64C-0.56Mn-0.37Si	755, 775, 806, 825
Fe-0.66C-1.06Mn-0.92Si	
Fe-0.68C-1.58Mn-1.33Si	

Each sample is electroplated with pure Fe (5-10µm) to minimize the effects of solute oxide on carbon removal.

Experimental results: Fe-0.74C-0.45Si (wt. %)



Interface model including 'solute-drag' [6]



$$J_X^1 = -\frac{D_X^1}{RT} x_{Fe}^0 x_X^0 \frac{(\mu_X^1 - \mu_X^0) - (\mu_{Fe}^1 - \mu_{Fe}^0)}{\delta}$$

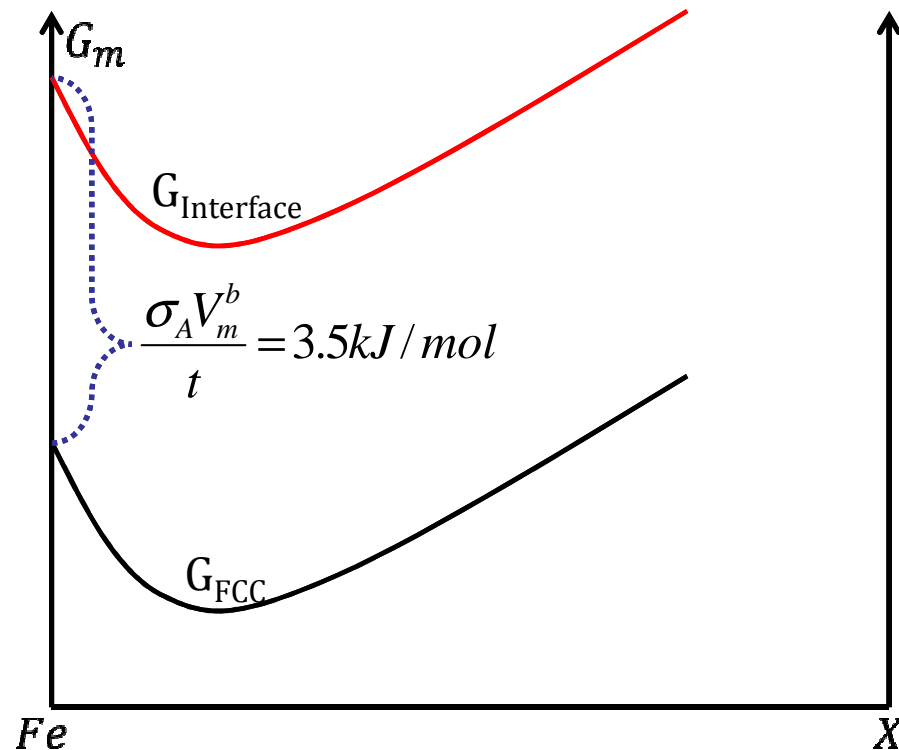
$$J_X^2 = -\frac{D_X^2}{RT} x_{Fe}^1 x_X^1 \frac{(\mu_X^2 - \mu_X^1) - (\mu_{Fe}^2 - \mu_{Fe}^1)}{\delta}$$

$$J_X^3 = -\frac{D_X^3}{RT} x_{Fe}^2 x_X^2 \frac{(\mu_X^3 - \mu_X^2) - (\mu_{Fe}^3 - \mu_{Fe}^2)}{\delta}$$

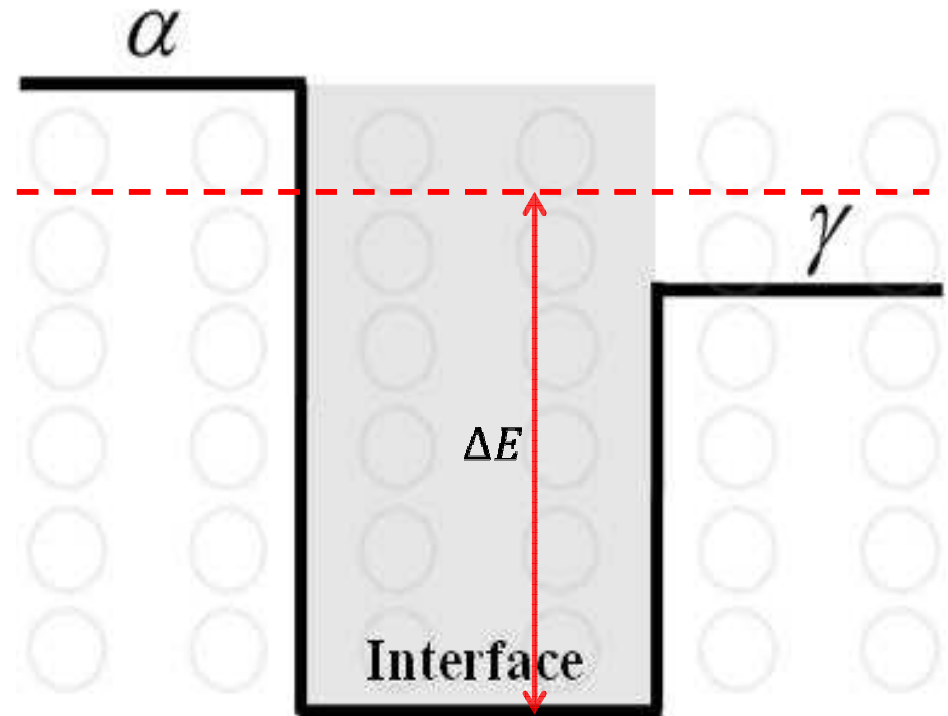
Hillert's expression for diffusional dissipation

$$\Delta G^{dissipated} = \sum_{i=1}^{i=3} -\frac{V_m}{v} \cdot J_X^i \cdot [(\mu_X^i - \mu_X^{i-1}) - (\mu_{Fe}^i - \mu_{Fe}^{i-1})]$$

Thermodynamic description of the interface ^[6]



The reference state for the free energy was shifted by 3.5kJ/mol to capture an interfacial energy of the order of 0.5 J/m².



The Fe-X interaction term is modified to provide a binding energy for X to the interface.

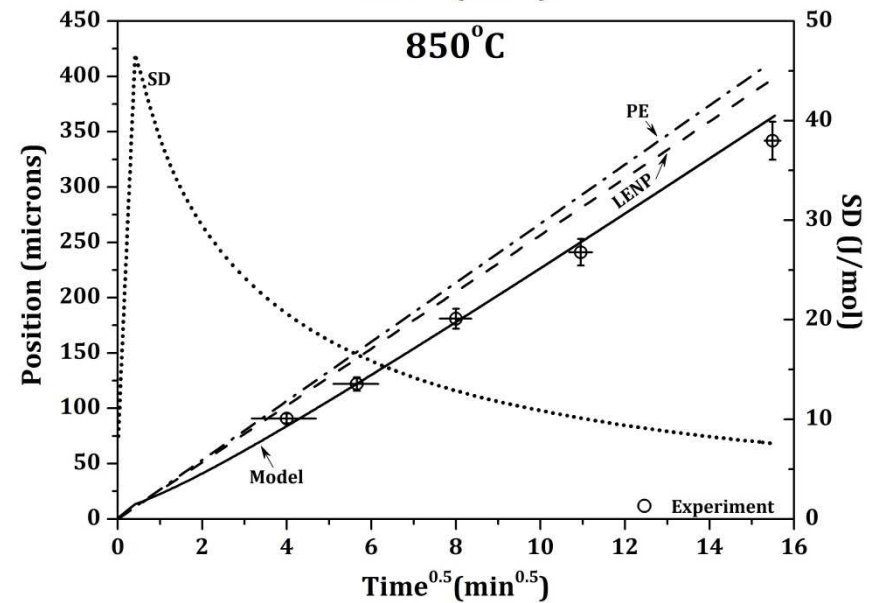
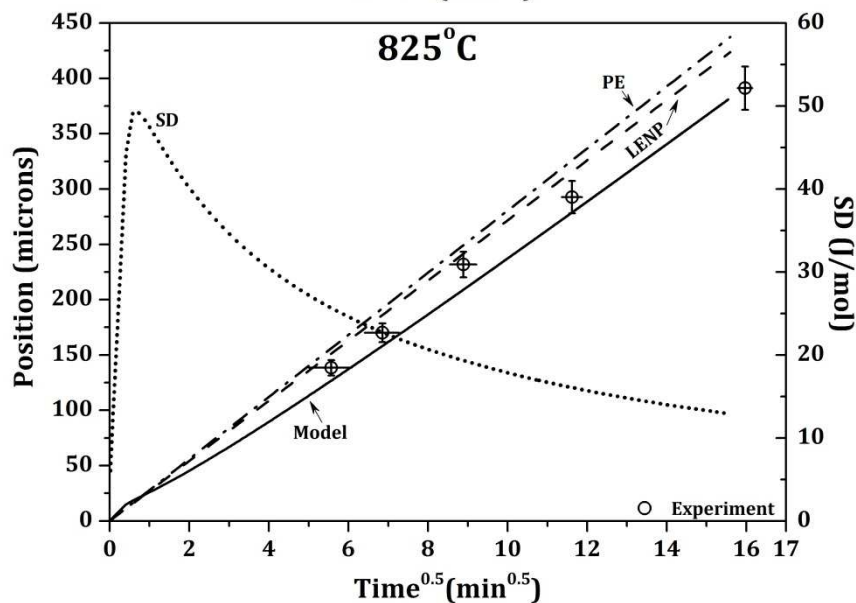
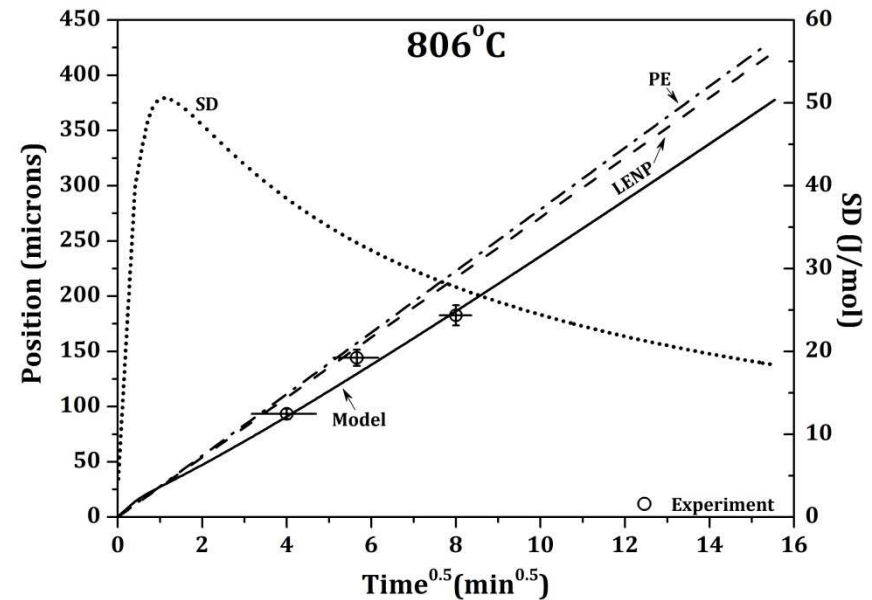
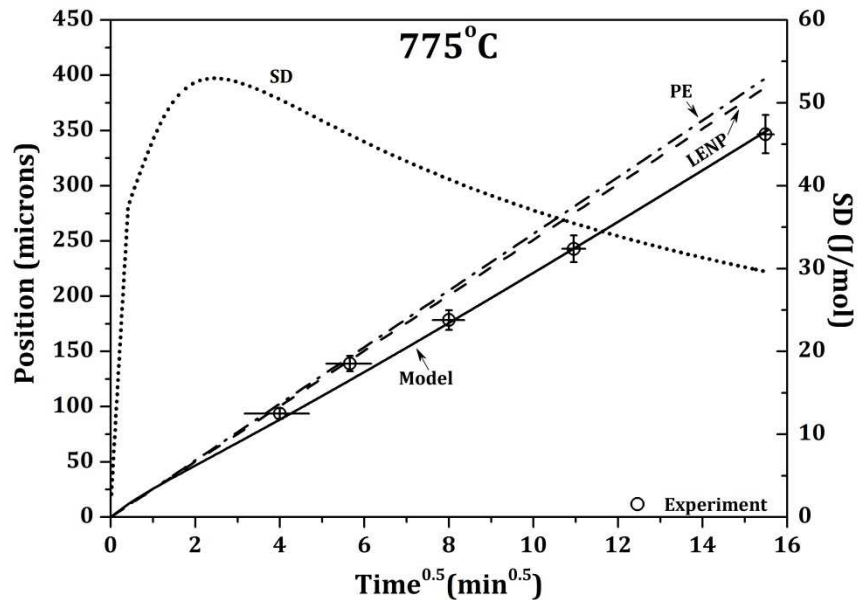
Interface parameters

Alloy	Binding energy (with respect to mid-point of Mn or Si chemical potential in ferrite and austenite)
Fe-C-Si	-9.0kJ/mol
Fe-C-Mn	-2.5kJ/mol

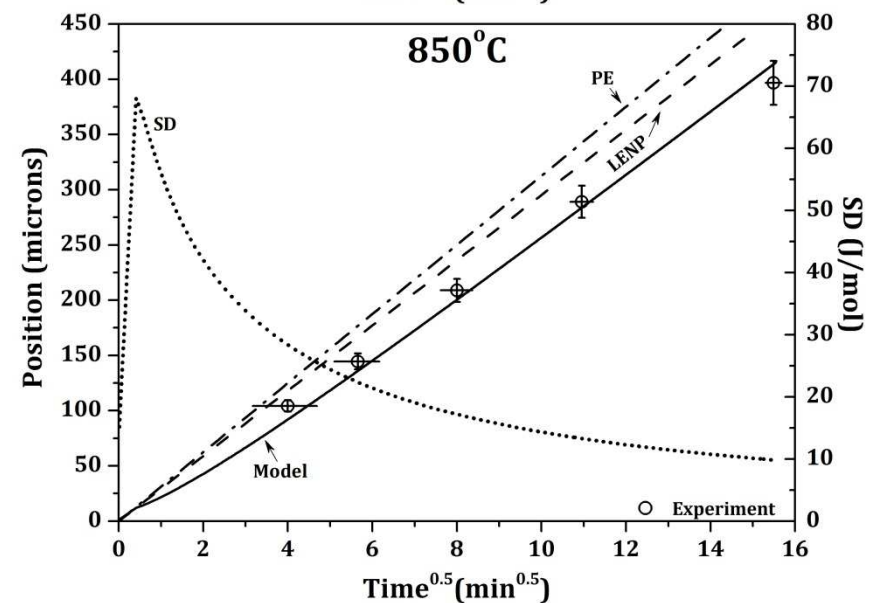
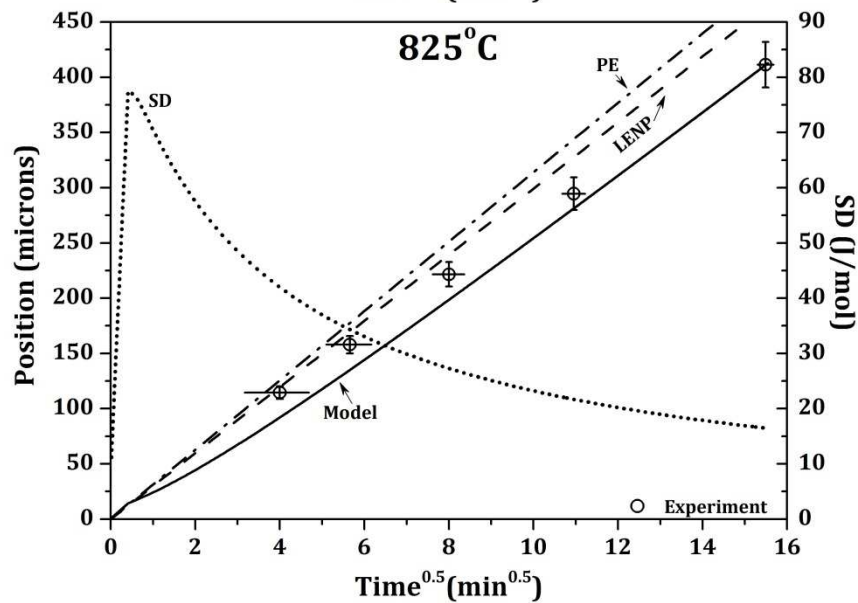
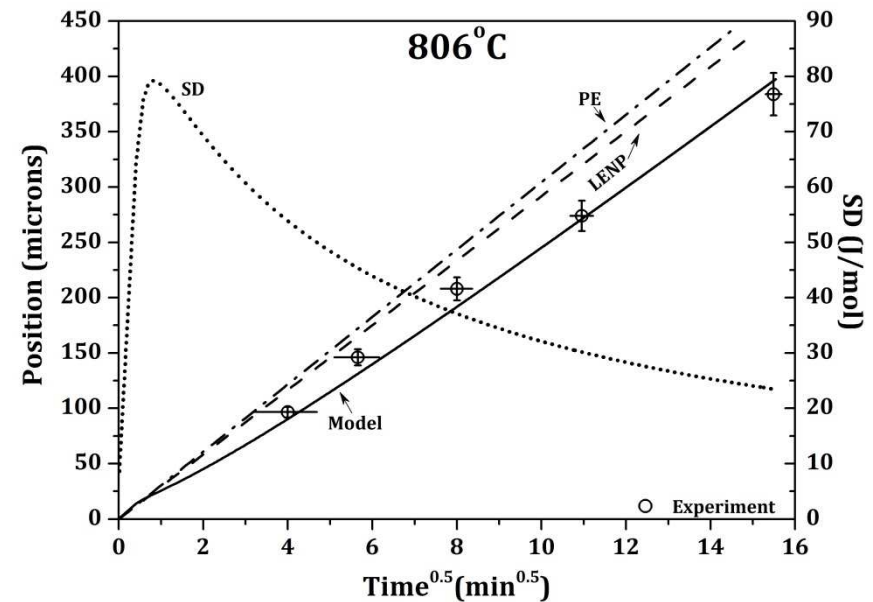
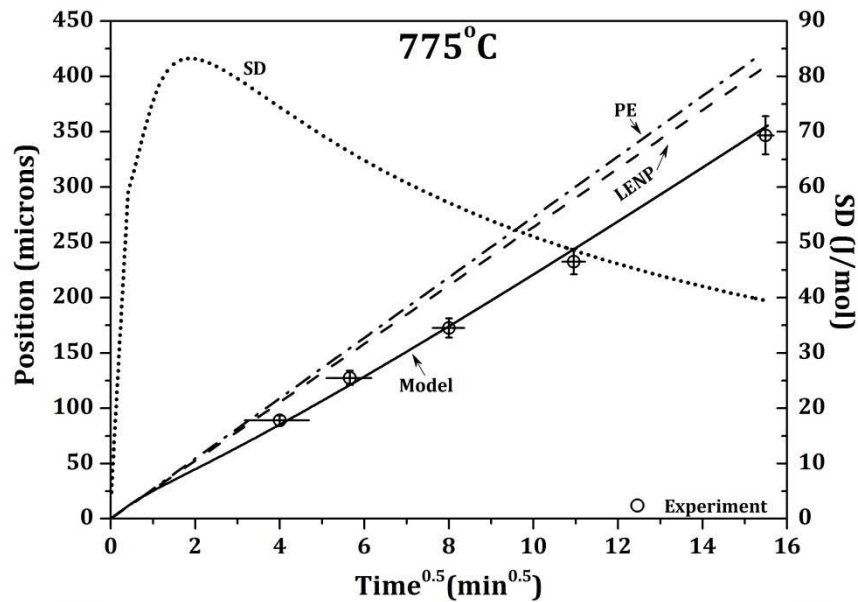
Alloy	D ₁	D ₂	D ₃
Fe-C-Si	Si Diffusivity in Ferrite	Si Diffusivity in Austenite	Si Diffusivity in Austenite
Fe-C-Mn	Mn Diffusivity in Ferrite	$\sqrt{D_1 \cdot D_2}$	Mn Diffusivity in Austenite

- Effect of solutes on carbon diffusivities in ferrite is also included (Dictra)

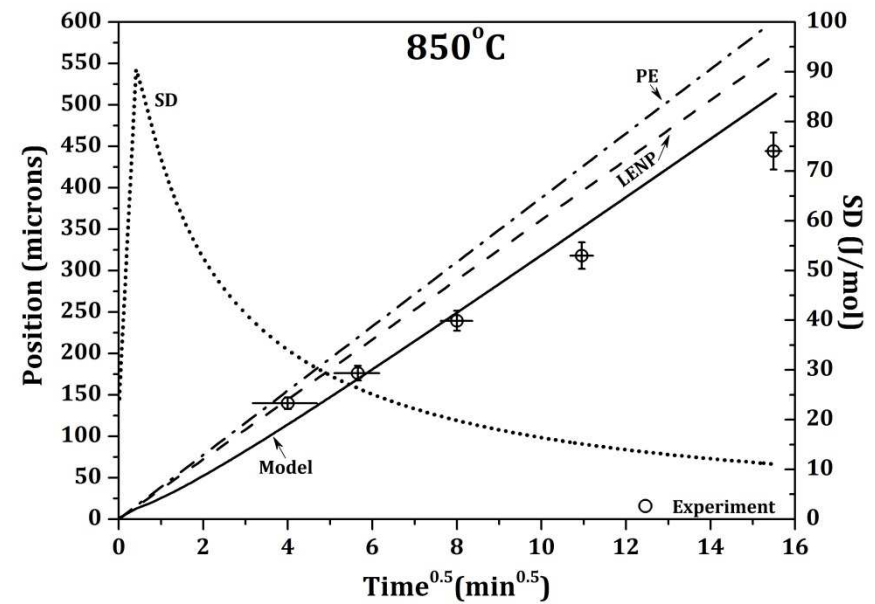
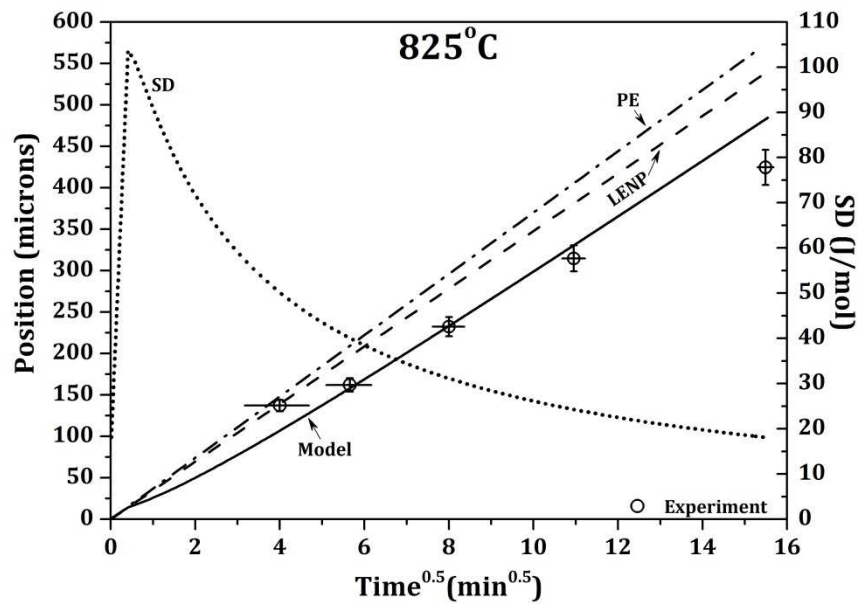
Ternary results: Fe-0.74C-0.45Si (wt. %)



Ternary results: Fe-0.76C-0.84Si (wt. %)



Ternary results: Fe-0.75C-1.46Si (wt. %)



Interface parameters

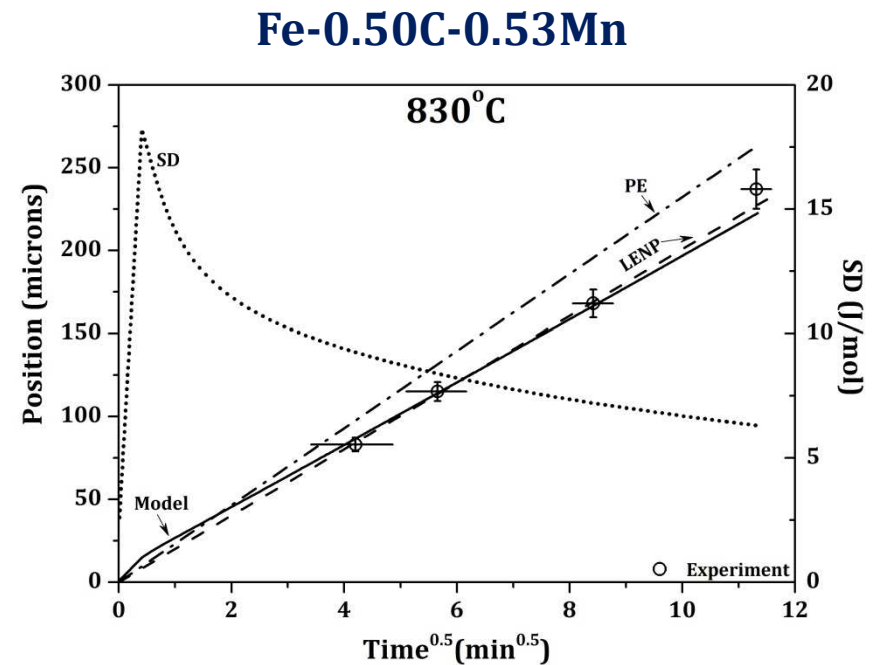
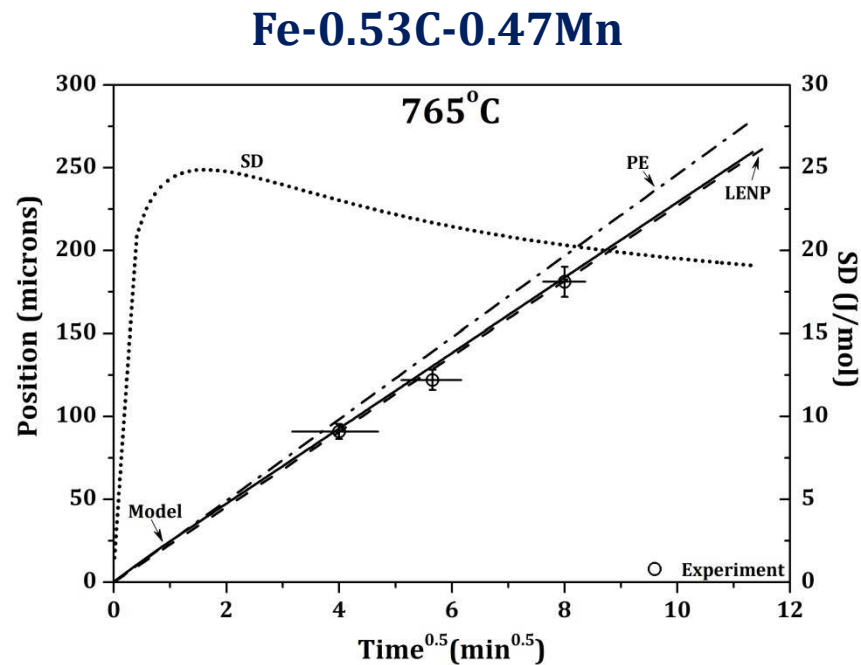
Alloy	Binding energy (with respect to mid-point of Mn or Si chemical potential in ferrite and austenite)
Fe-C-Si	-9.0kJ/mol
Fe-C-Mn	-2.5kJ/mol

Alloy	D ₁	D ₂	D ₃
Fe-C-Si	Si Diffusivity in Ferrite	Si Diffusivity in Austenite	Si Diffusivity in Austenite
Fe-C-Mn	Mn Diffusivity in Ferrite	$\sqrt{D_1 \cdot D_2}$	Mn Diffusivity in Austenite

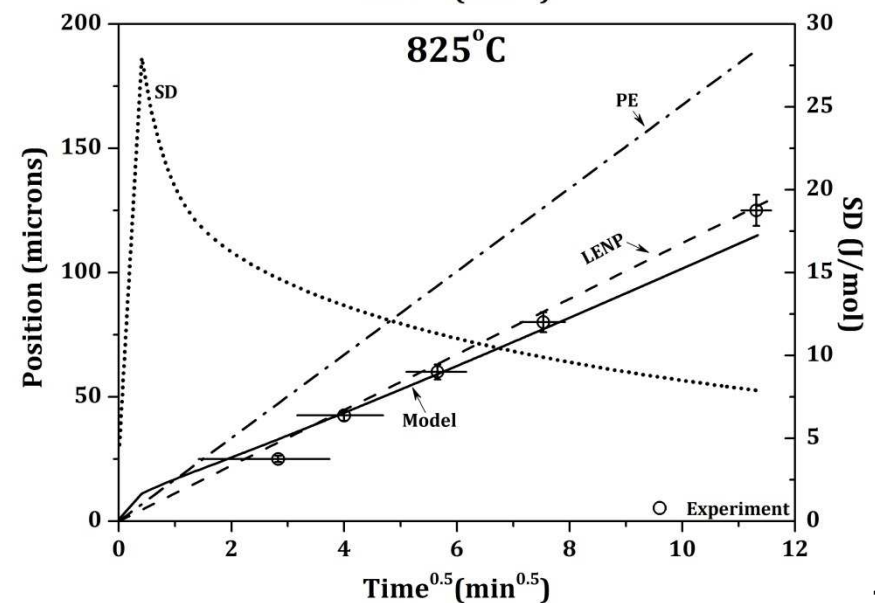
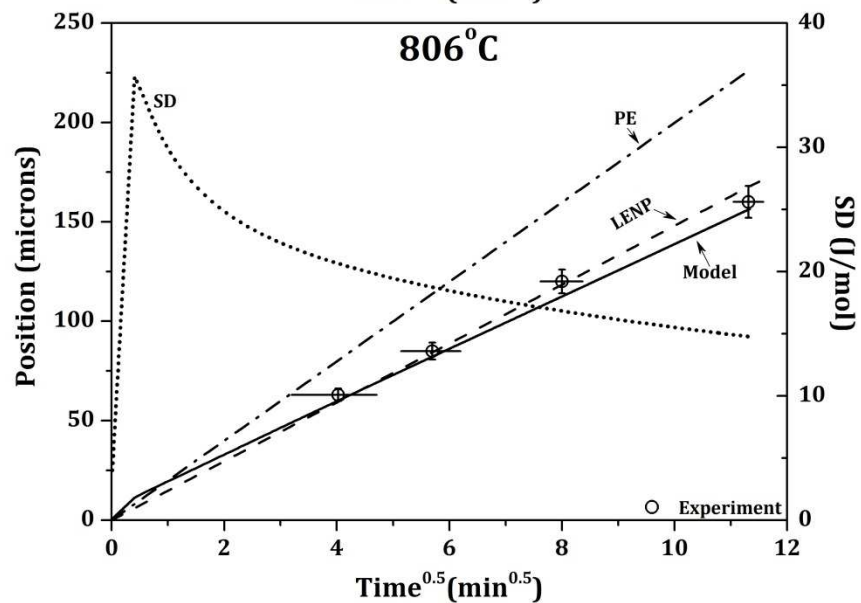
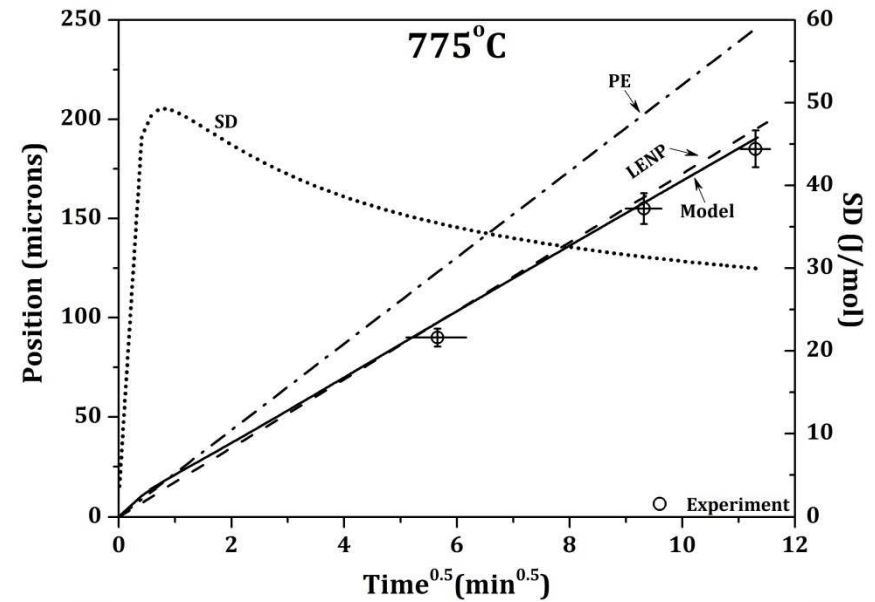
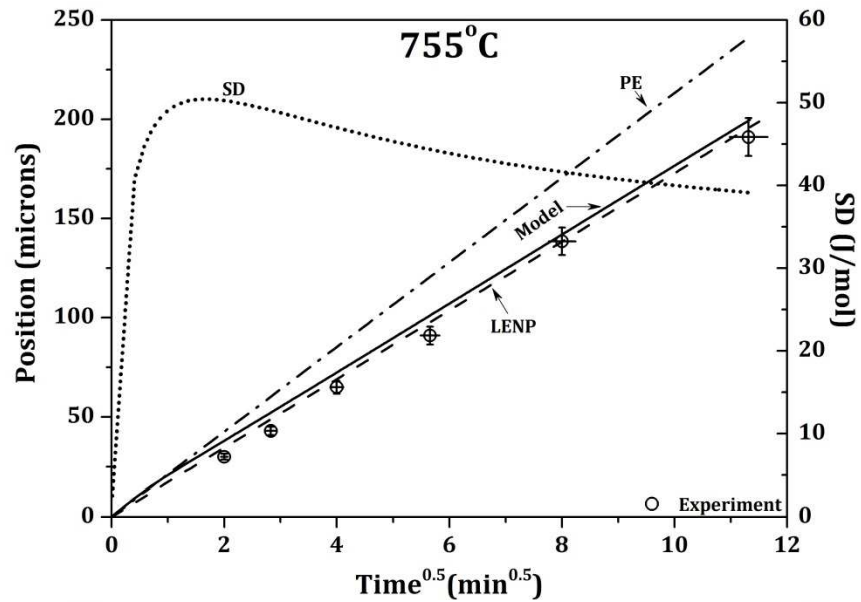
- Effect of solutes on carbon diffusivities in ferrite is also included (Dictra)
- The thermodynamic expressions for ferrite and austenite in Fe-C-Mn system are modified for more accurate thermodynamic description:

$$L(\text{BCC,Fe,Mn:Va;0})=+20768.8-20.97 \cdot T^{[2]} \quad L(\text{FCC,Fe,Mn:Va;0})=+11758-13.89 \cdot T^{[6]}$$

Ternary results: Fe-0.5C-0.5Mn (wt. %)



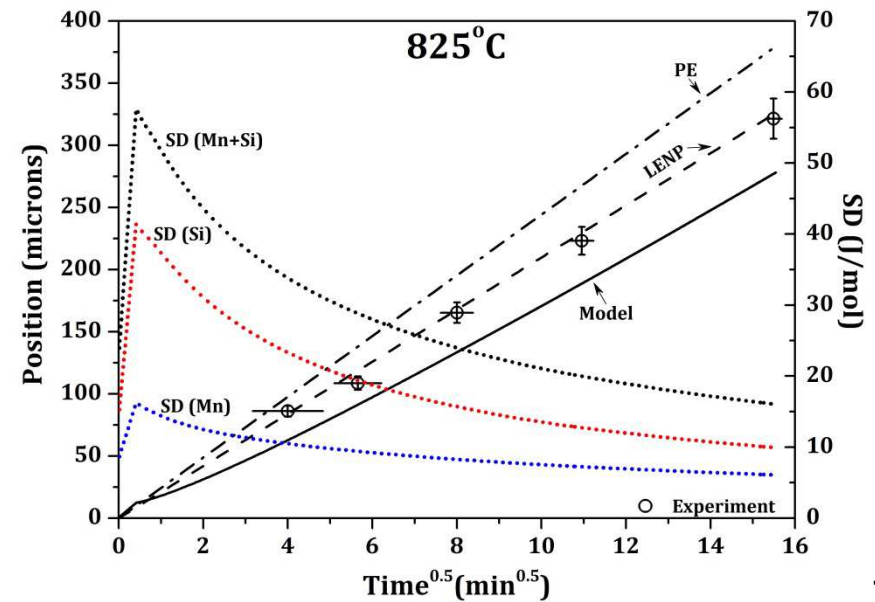
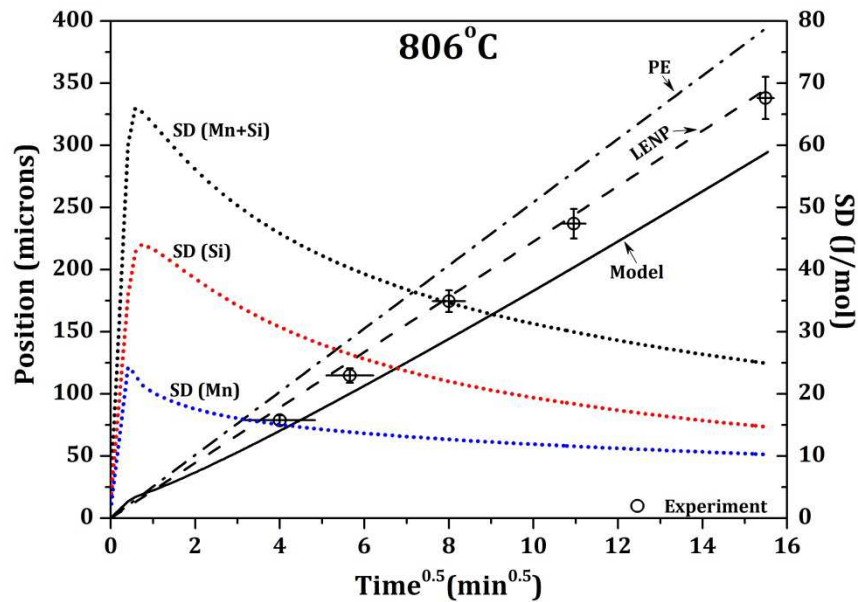
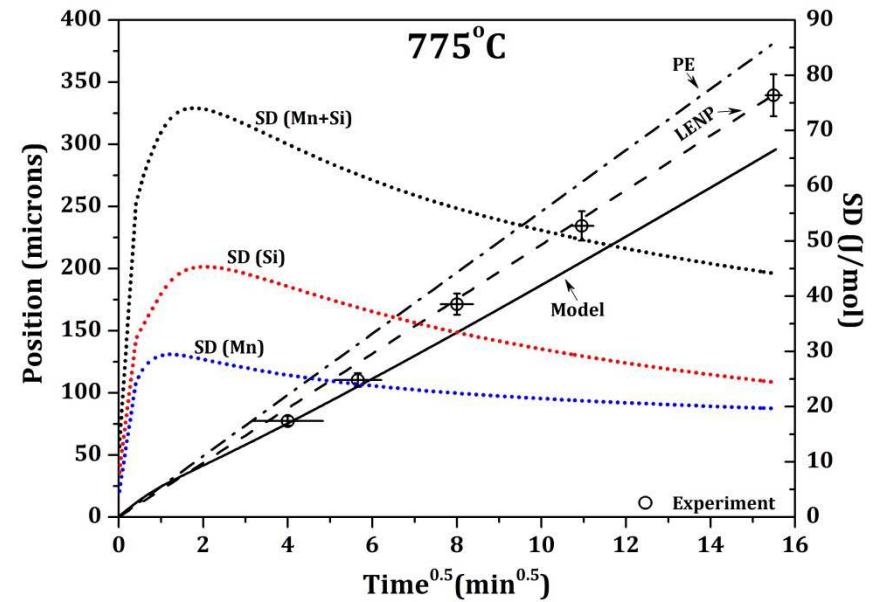
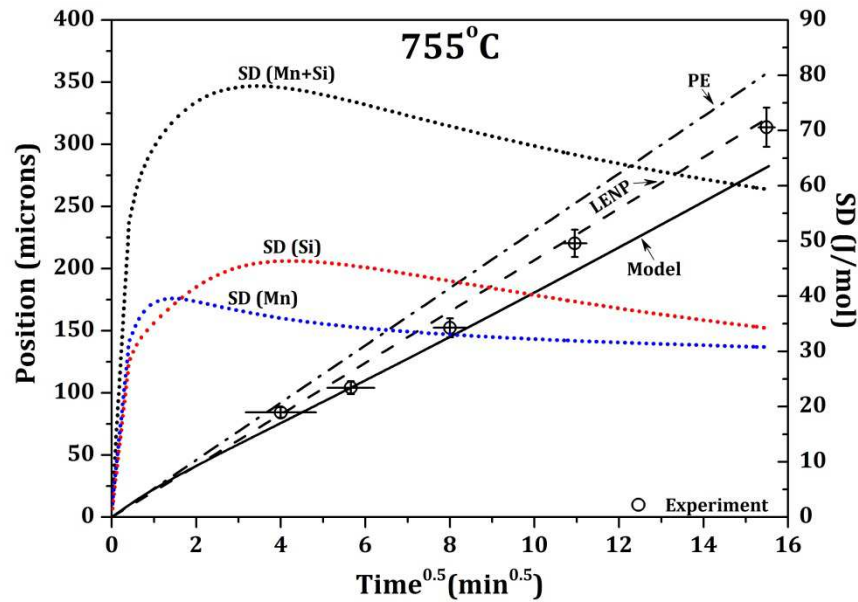
Ternary results: Fe-0.57C-0.94Mn (wt. %)



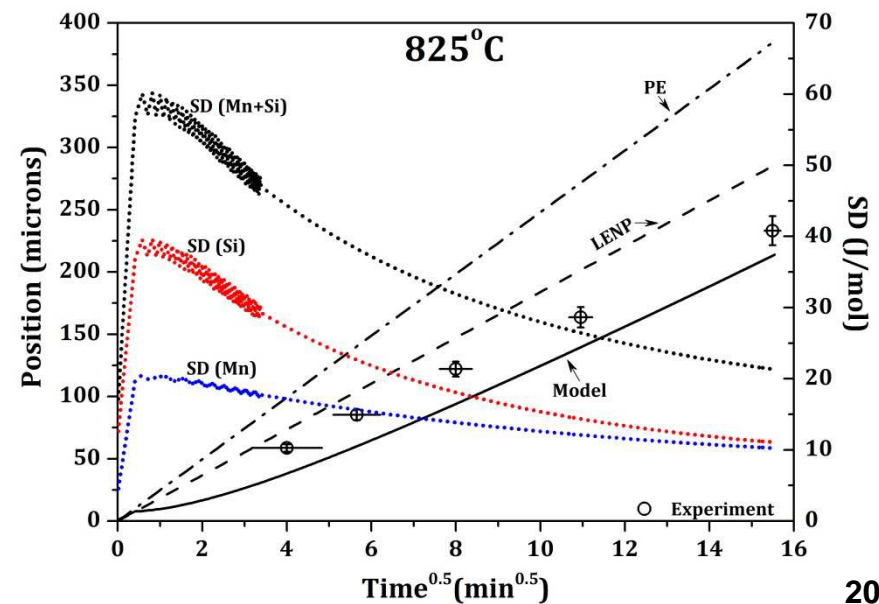
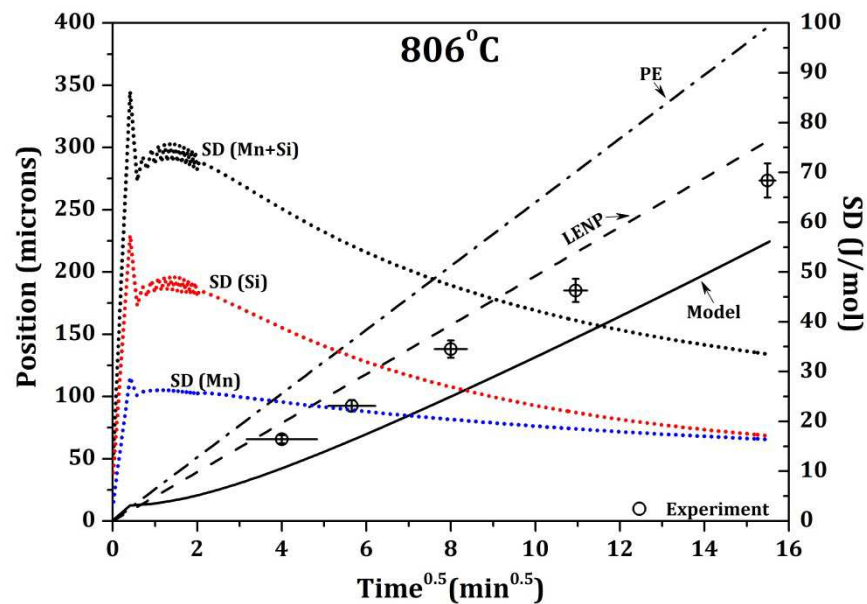
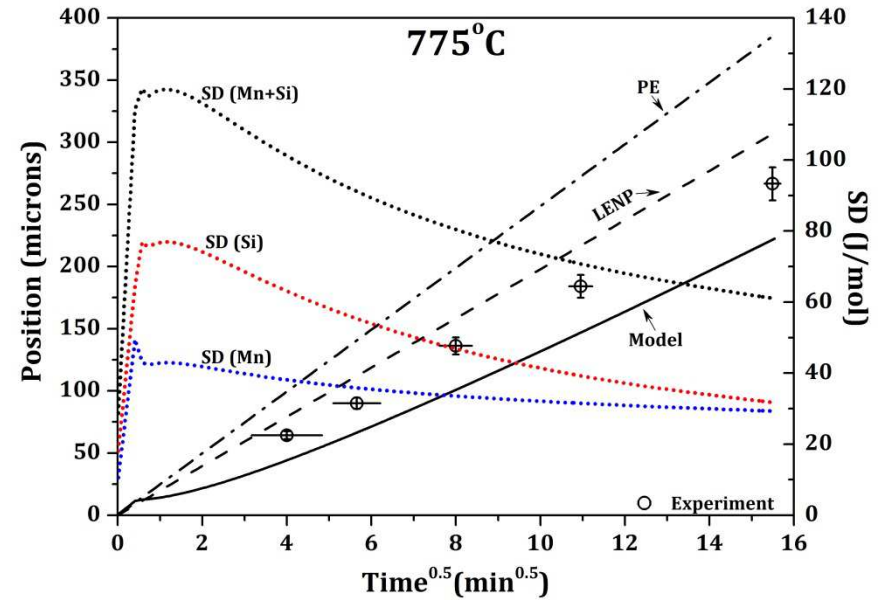
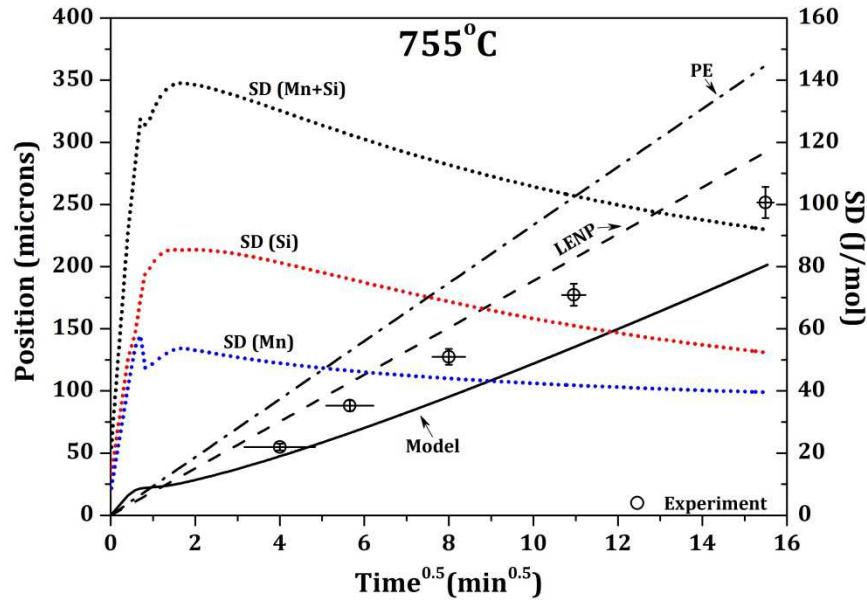
Extension to Fe-C-Mn-Si quaternary system

- Solute binding energies and trans-interface diffusivities calibrated from the ternary systems are used to test how well the kinetics in the quaternary systems are predicted.
- Two conditions are examined:
 - The interaction between Mn & Si in the interface is the same as that in Austenite (ie. C-SDE exists)
 - No interaction between Mn & Si in the interface

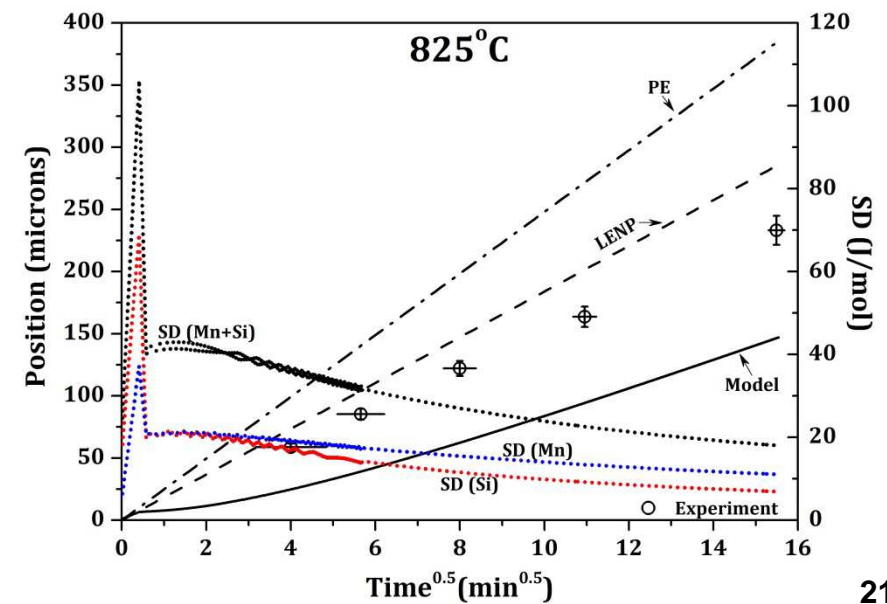
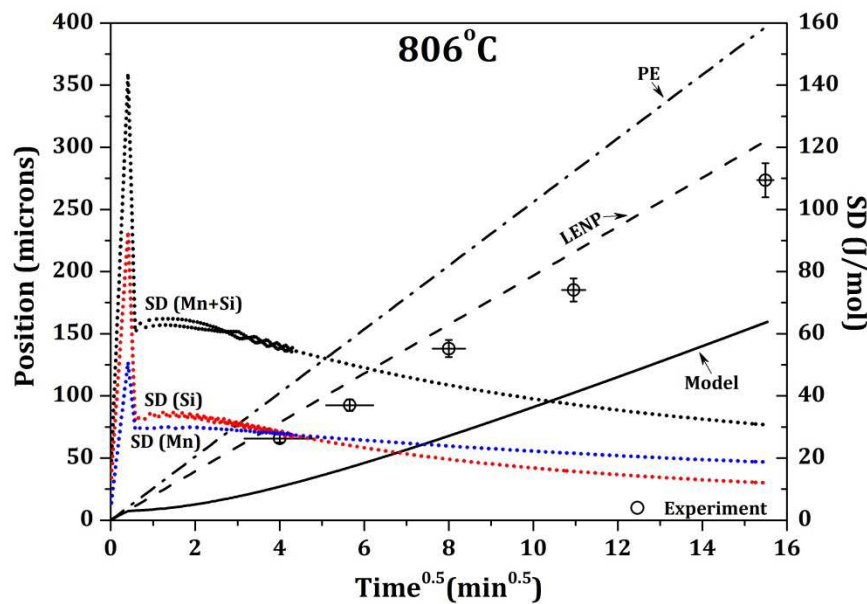
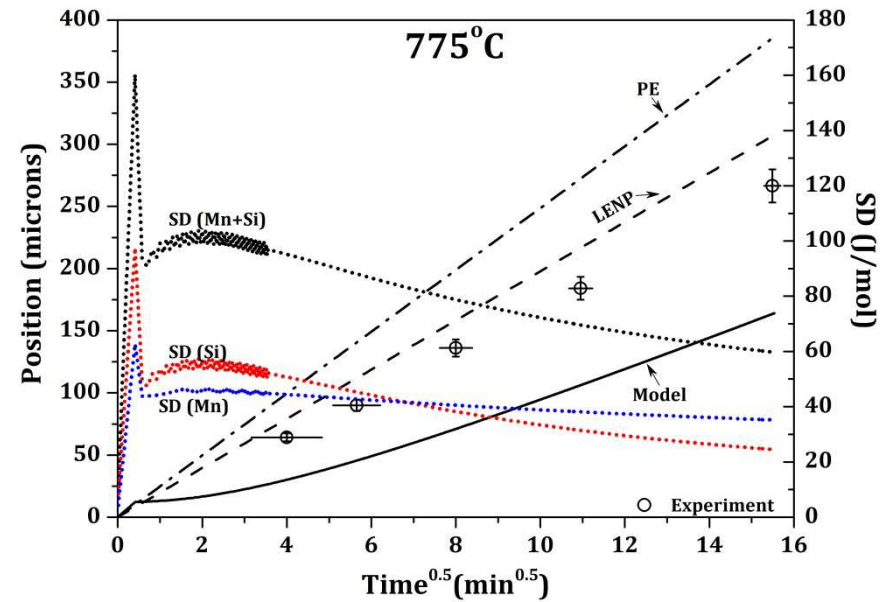
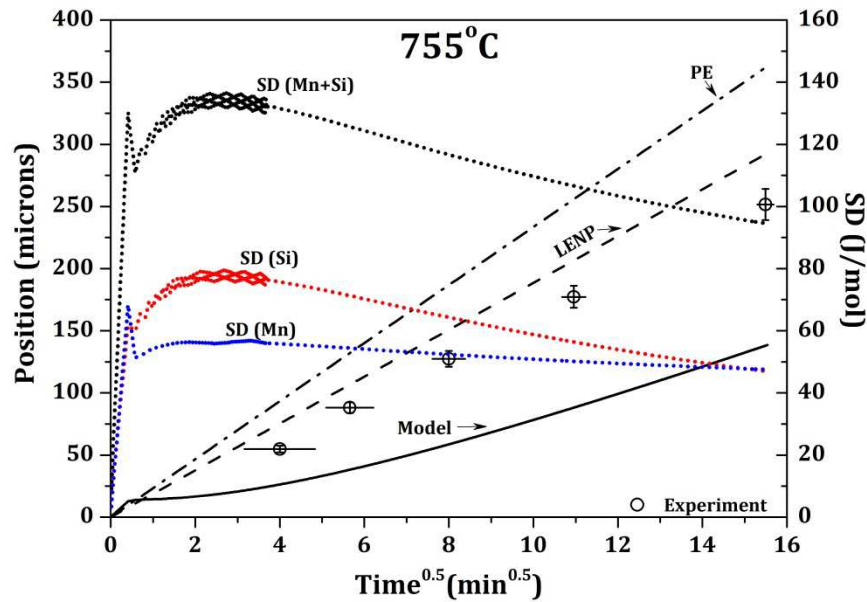
$(\text{Mn:Si})^I = (\text{Mn:Si})^V$ for Fe-0.64C-0.56Mn-0.37Si (wt. %)



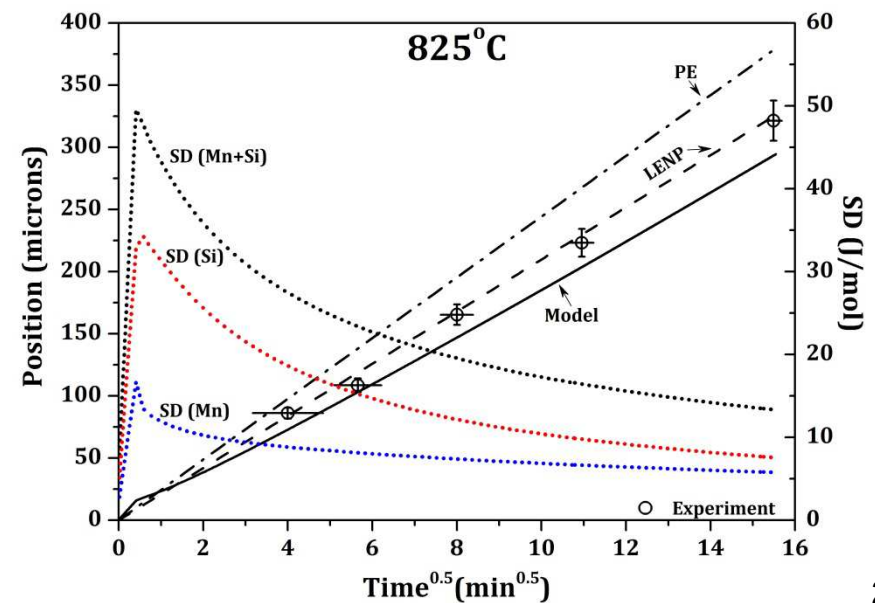
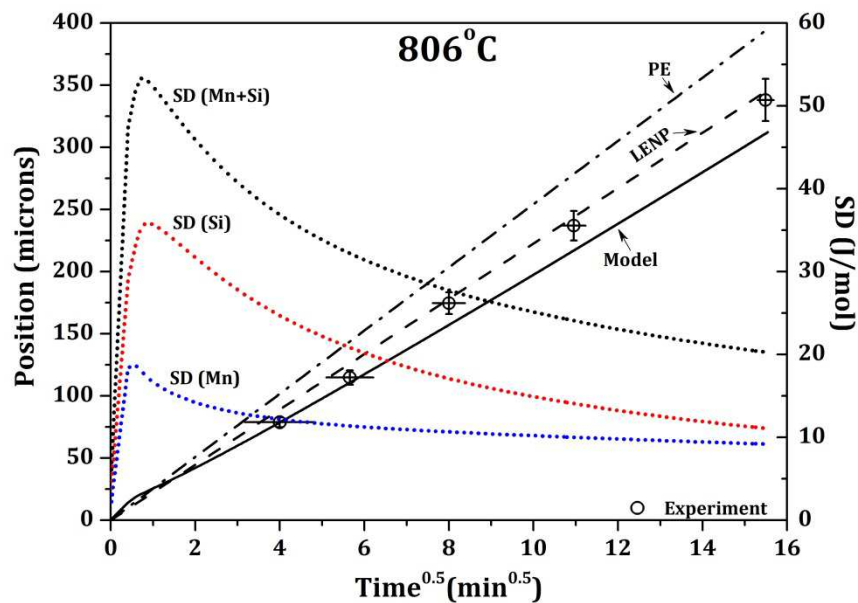
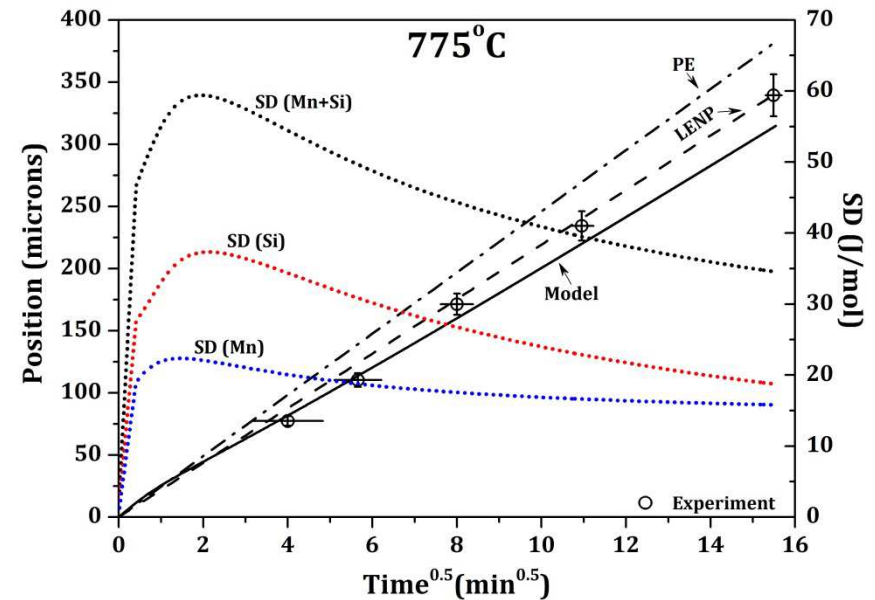
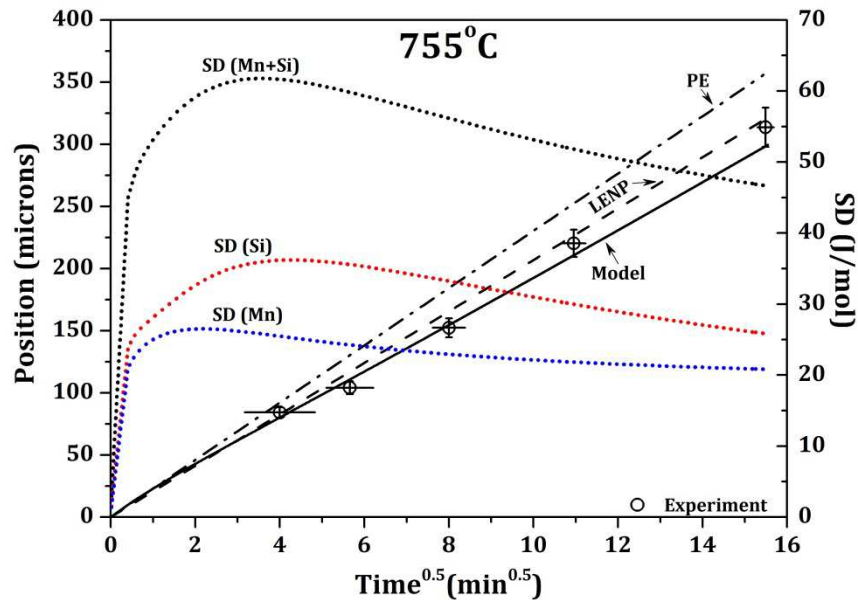
$(\text{Mn:Si})^I = (\text{Mn:Si})^V$ for Fe-0.66C-1.06Mn-0.92Si (wt. %)



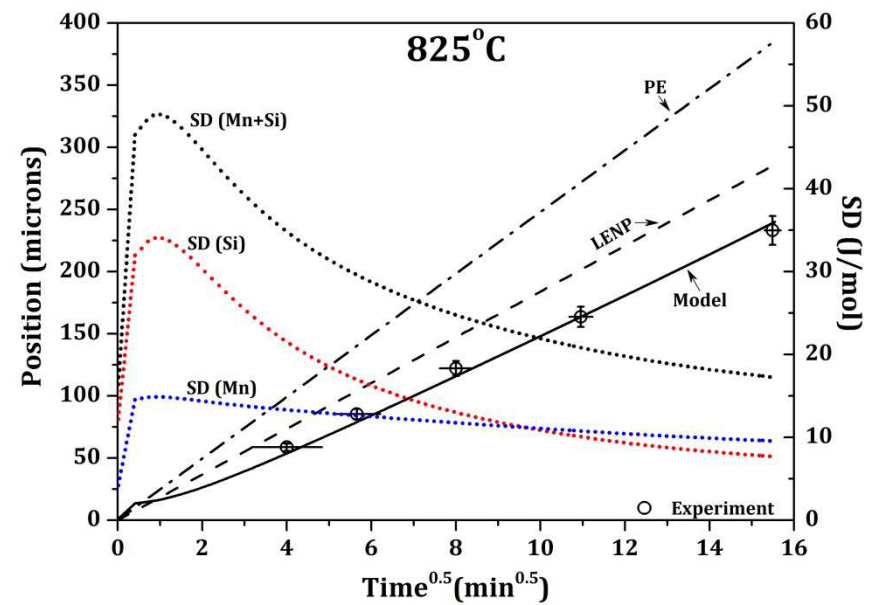
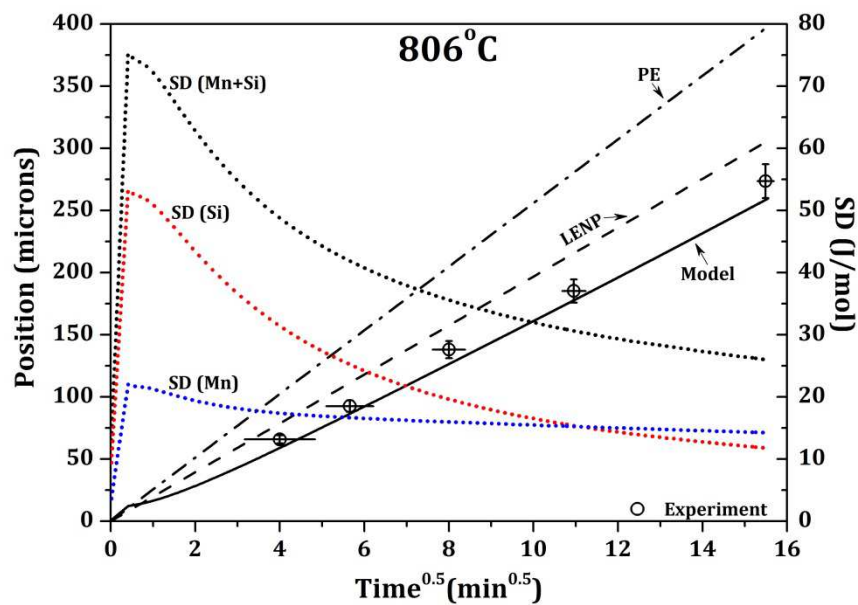
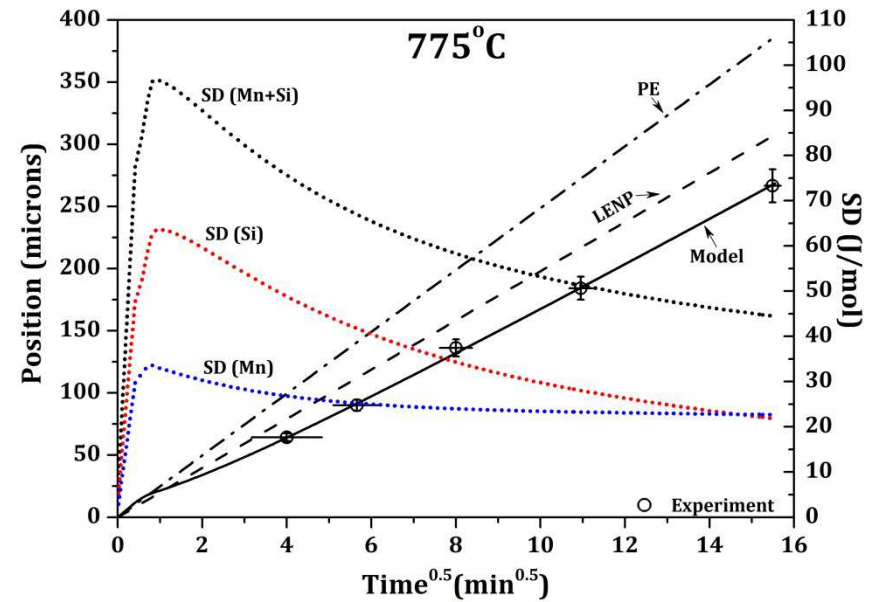
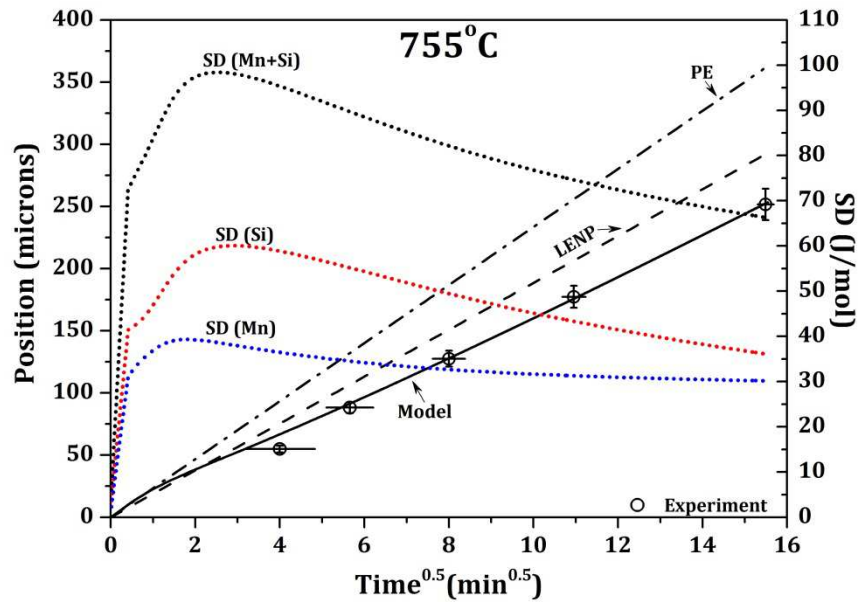
$(\text{Mn:Si})^I = (\text{Mn:Si})^V$ for Fe-0.68C-1.58Mn-1.33Si (wt. %)



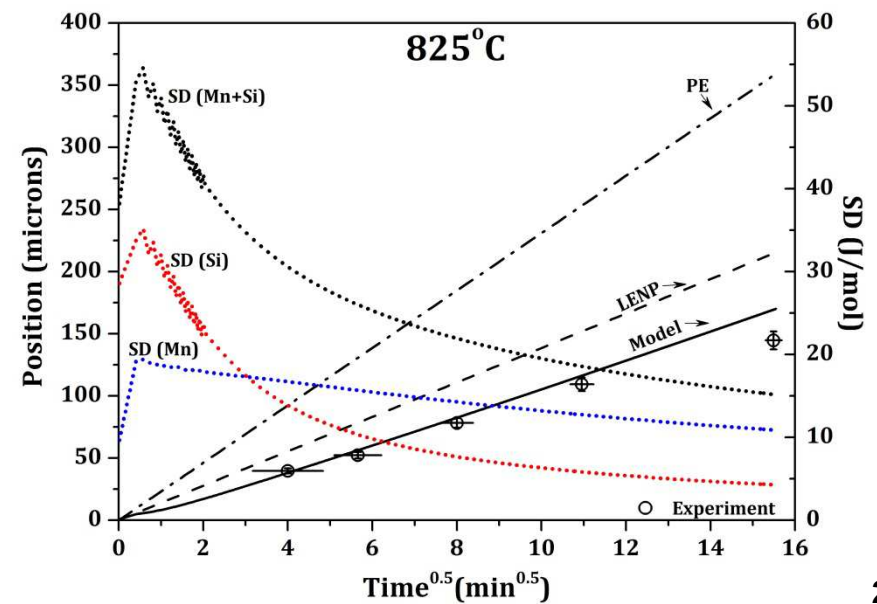
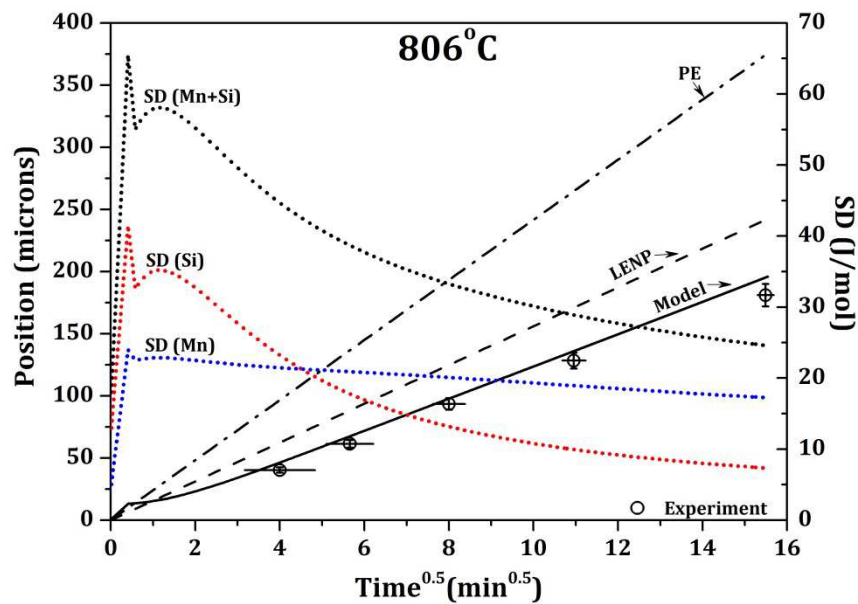
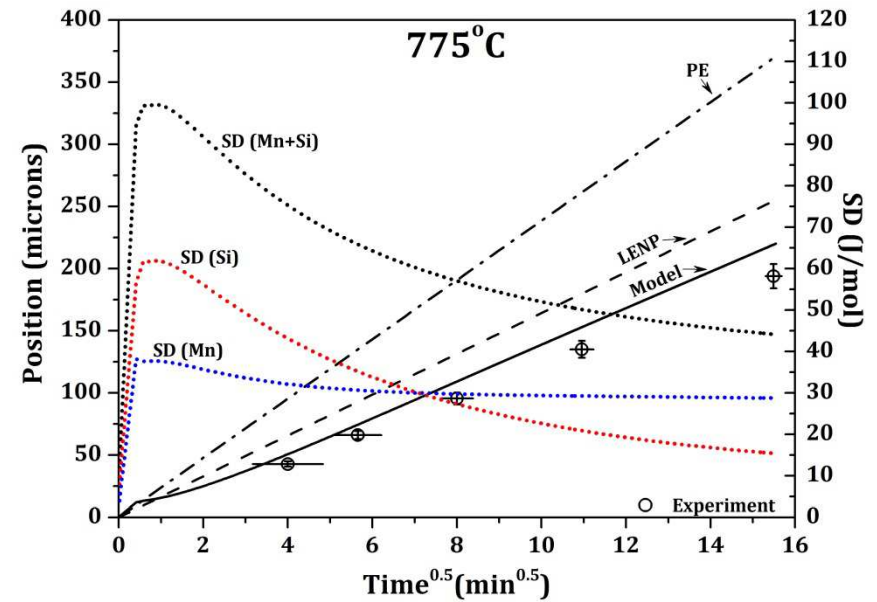
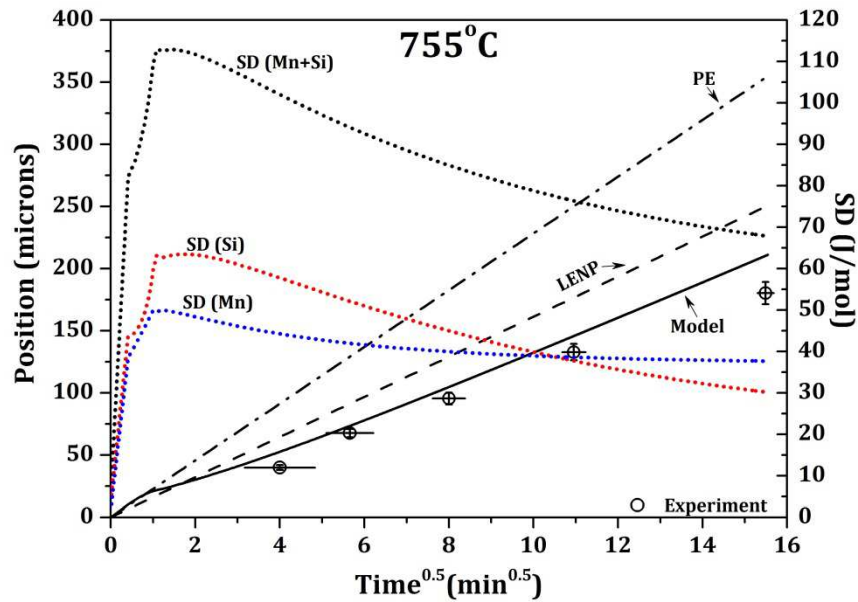
$(\text{Mn:Si})^I=0$ for Fe-0.64C-0.56Mn-0.37Si (wt. %)



$(\text{Mn:Si})^I=0$ for Fe-0.66C-1.06Mn-0.92Si (wt. %)



$(\text{Mn:Si})^I = 0$ for Fe-0.68C-1.58Mn-1.33Si (wt. %)



Summary

- Ferrite growth kinetics of Fe-C-Mn-Si alloys can be reasonably well described using parameters tuned from ternary systems
- For the velocities encountered in decarb experiments, the kinetics of ferrite growth in Fe-C-Mn-Si are well described using no interaction between Mn and Si in the interface.

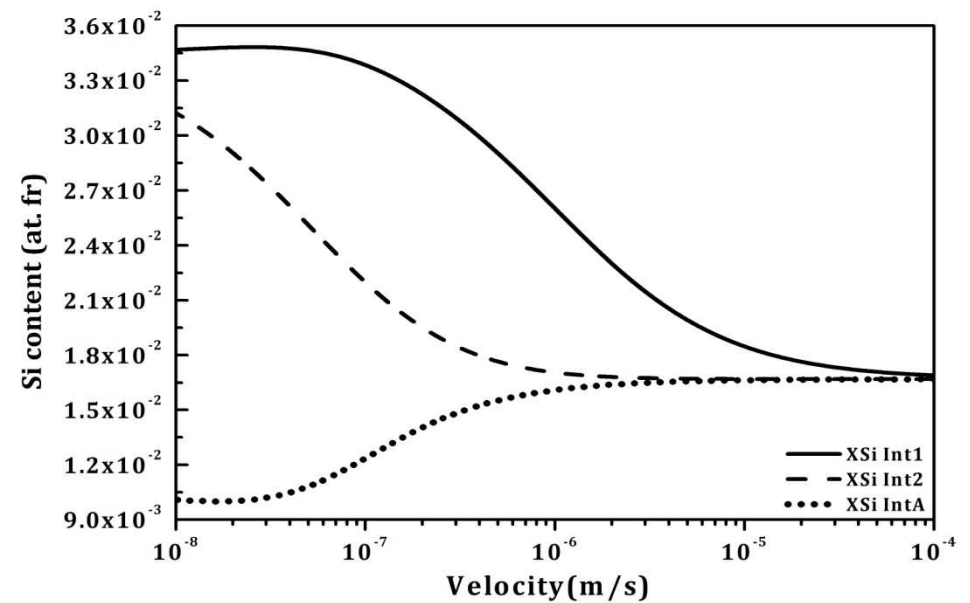
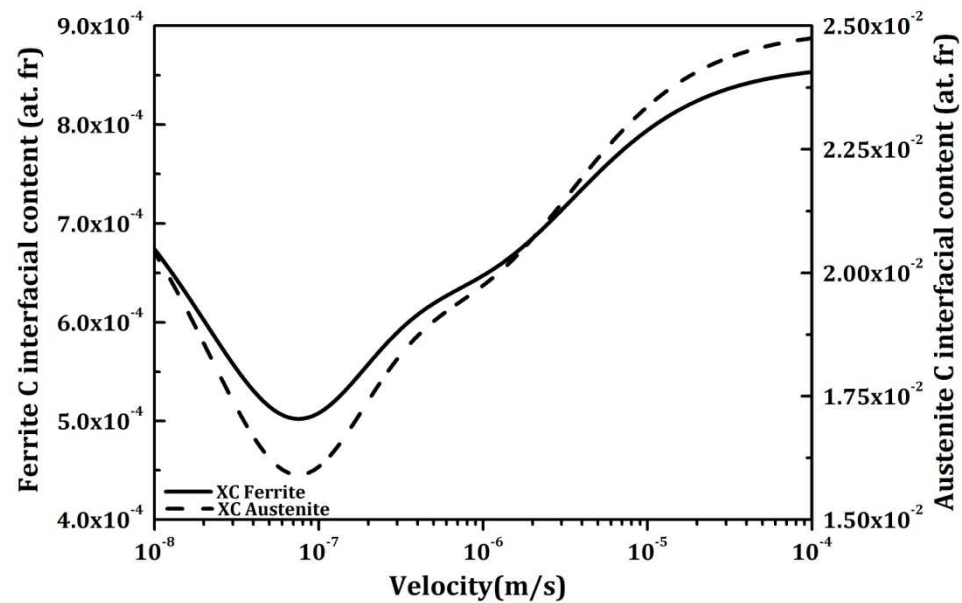
Discussion Points

A suitable method to select the binding energy and cross-interface diffusivities (fga for Mn & faa for Si?) remains unresolved.

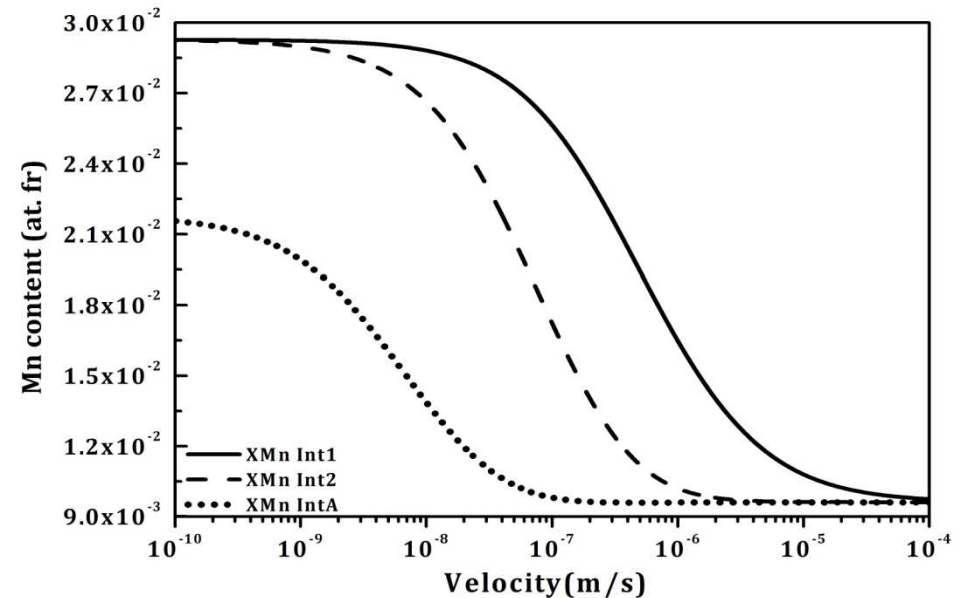
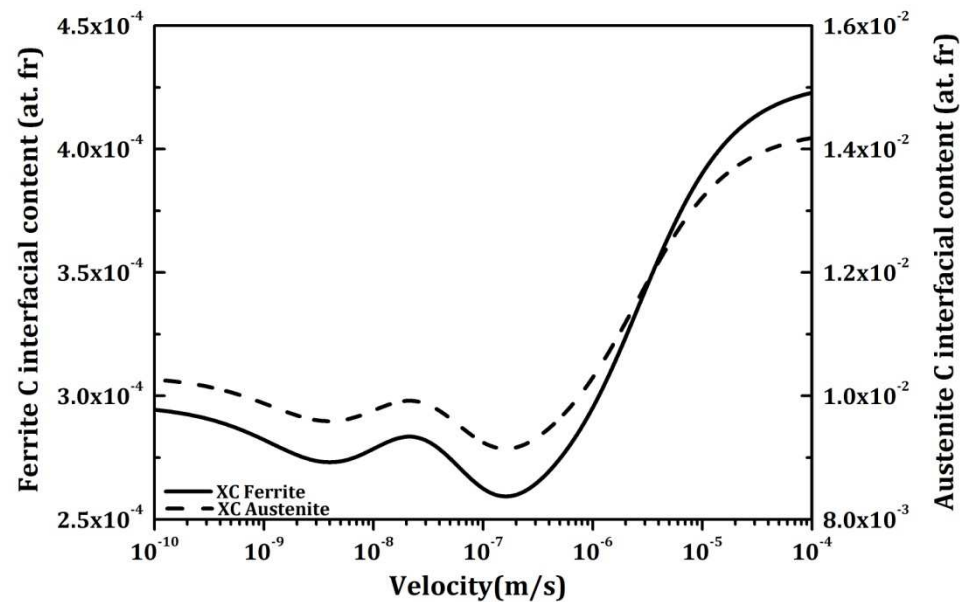
In Fe-C-Mn, the kinetics agree perfectly with LENP. It may seem too much of a coincidence for SD to be exactly the correct magnitude to give this overall effect.

The question of summing SD from different elements may require discussion ($SD = SD(Mn) + SD(Si)$, $SD = \text{largest of } SD(Mn) \text{ or } SD(Si)$?, etc.)

Interfacial Compositions: Fe-0.76C-0.84Si (wt. %) at 775°C



Interfacial Compositions: Fe-0.57C-0.94Mn (wt. %) at 775°C



Interfacial Compositions for $(\text{Mn:Si})^I=0$: Fe-0.66C-1.06Mn-0.92Si at 775°C

